Low Noise Figure, Wide Bandwidth Analog Optical Link

Edward Ackerman, Gary Betts, William Burns, Joelle Prince, Michael Regan, Harold Roussell, and Charles Cox

Photonic Systems, Inc., 900 Middlesex Turnpike, Building # 5, Billerica, MA 01821, USA

***Abstract* — We report achieving a record low noise figure for an amplifierless fiber-optic link — ≤ 15 dB over the frequency range 1.0 – 9.5 GHz — via a combination of a low-V_{π} Mach-Zehnder modulator with two antiphase outputs, a high-power laser, and a balanced photodetector pair. We also present a complete model for this link that predicts its measured performance to within 1 dB.**

***Index Terms* — bandwidth, modeling, noise figure, optical communication, optical modulation.**

I. Introduction

Noise figure is one of the key parameters in analog optical links intended for antenna remoting applications. In general, low noise figure can be achieved in one of two ways. One approach is to design the intrinsic link (*i.e.*, the link without any RF amplification) to have the required low noise figure. As Fig. 1 shows, to date this has been possible only at low frequencies and over relatively narrow bandwidths. For example, in 1998 one of us (Prince) achieved a noise figure of < 4 dB across a bandwidth of ~ 30 – 50 MHz (see Fig. 5.10 in [1]). By adjusting the RF match at the input end of a link for minimum noise figure rather than maximum gain, noise figure was reduced to 2.5 dB in a very narrow bandwidth around 130 MHz [2].

Because intrinsic links usually do not have sufficiently low noise figure for many applications, most analog link designers have achieved low noise figure using the second general approach: augmenting the intrinsic link with a low-noise RF preamplifier. In principle it is possible to reduce any noise figure to an arbitrarily low value by preceding the link with an RF amplifier that has the required low noise figure and sufficiently high gain to make the intrinsic link's contribution to the overall noise figure negligible.

There are at least two major drawbacks to this second approach. One is fundamental: the high-gain pre-amplifier needs to also have a high intercept point, to avoid degrading the spurious-free dynamic range of the link. The other drawback is practical: an amplifier with sufficiently high gain and low noise figure may be unavailable, especially in the case of links with high center frequency and/or broad bandwidth.

Hence it is important to minimize the noise figure of the intrinsic link. To date the link having the lowest noise figure over the widest bandwidth of which we are aware was demonstrated by Williams *et al.*, who achieved a noise figure of 16.5 dB over a bandwidth extending from baseband up to 3 GHz [3].

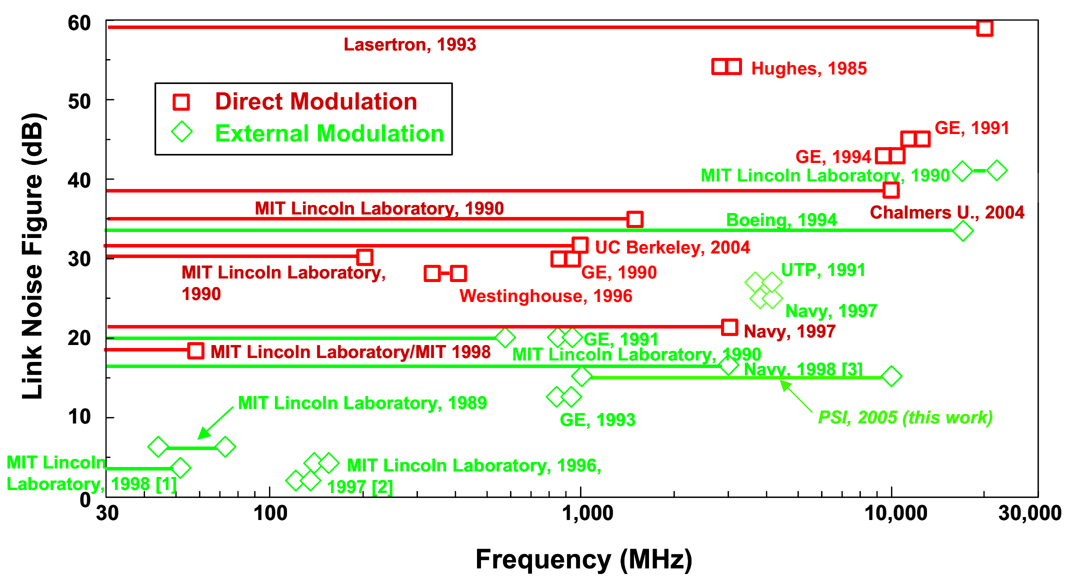

Fig. 1 Measured noise figures of intrinsic direct and external modulation analog optical links.

ISBN 89-950043-3-9 93560

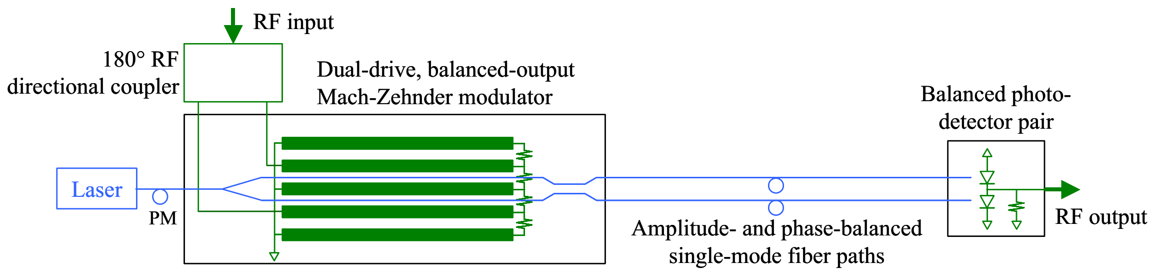

Fig. 2 Block diagram experimental analog optical link with low intrinsic noise figure.

In this paper we report on the design and implementation of an optical link in which we have been able to achieve a low noise figure over a wide bandwidth. We achieved these results by combining components with unusually good performance—especially in the case of the modulator—in a link architecture that uses two balanced paths between the modulator and photodetector to maximize signal-to-noise performance.

II. Link Performance Model

A block diagram of the link is shown in Fig. 2. For the sake of simplicity, operational aspects needed to support these components, such as power supplies and bias controllers used in the experiment are not shown. The link consists of a laser whose output is coupled via polarization maintaining fiber into a Mach-Zehnder modulator with two balanced single-mode fiber outputs. In this balanced Mach-Zehnder, the two phase-modulated arms of the interferometer are combined in an optical directional coupler such that the two modulated optical outputs have intensity modulation with the same amplitude but differing in RF phase by 180°. These two optical output fibers are connected to runs of single-mode fiber that are matched to one another in terms of incurred loss and RF delay, and at the far end of these fiber runs they are connected to the length-matched input fiber pigtails of a commercial balanced photodetector pair.

The noise figure, *NF*, of the link depicted in Fig. 2 can be written as

$$NF = 10\log\left[1 + x(f) + \frac{R_{LOAD}}{g_i\, k\, T}\left(\overline{i_{RIN}^2} + \overline{i_{sn}^2} + \overline{i_{tn}^2}\right)\right], \quad (1)$$

where the total current spectral density of the noise fed to the output load R_{LOAD} arises from the photodetected relative intensity noise (*RIN*) of the laser, the photodetectors' shot noise (*sn*), and the photodetector circuit's thermal noise (*tn*), and where k is Boltzmann's constant and $T_0 \equiv 290$ K. The term $x(f)$ in (1) reflects the degree to which thermal noise generated by the modulator electrode termination impedance, and by ohmic losses in the electrodes themselves, contributes to *NF*. This term has been derived previously [4]:

$$x(f) = \frac{\sin^2(2\pi f\tau)}{(2\pi f\tau)^2} + \left(\frac{\alpha L}{1-e^{-\alpha L}}\right)^2\left(1 + \frac{2}{\alpha L}\left[-\sqrt{1-e^{-\alpha L}} + \ln\left(1+\sqrt{1-e^{-\alpha L}}\right)\right]\right)^2. \quad (2)$$

In (2), α is the attenuation along the modulator's traveling-wave electrodes, and $\tau = nL/c$, where n and L are the electrodes' microwave index (assumed to be matched to the optical index) and length, and c is the speed of light *in vacuo*. For any frequency at which the electrode design permits efficient modulation of the light, it is likely that $x(f) < 1$; this term therefore usually has only a small effect on *NF*. It is more common for the *RIN*, shot noise, or detector thermal noise terms to dominate the link *NF*. For resistively matched balanced photodiodes illuminated by the outputs of a balanced Mach-Zehnder modulator, the three noise current densities in (1) are:

$$\overline{i_{RIN}^2} = \left(\frac{I_D}{2}\right)^2 RIN\left(1+\rho^2-2\rho\cos\phi\right)\left|H_{D,dev}(f)\right|^2\left|H_{D,pkg}(f)\right|^2, \quad (3)$$

$$\overline{i_{sn}^2} = \frac{1}{2}(1+\rho)\,q\,I_D\left|H_{D,pkg}(f)\right|^2, \quad \text{and} \quad (4)$$

$$\overline{i_{tn}^2} = \frac{kT}{R_{LOAD}}, \quad (5)$$

where $H_{D,dev}(f)$ and $H_{D,pkg}(f)$ are the frequency response of the photodetectors themselves and the additional roll-off due to the packaged balancing circuit (including its RF connector, bias tee, and any associated parasitic circuit elements), respectively, and q is the electronic charge. When the modulator is operated at its quadrature bias point, I_D, the larger of the two photodetectors' average currents, is calculated as follows:

$$I_D = \frac{1}{2}T_{FF}\,P_I\,r_d\,, \quad (6)$$

where T_{FF} is the fiber-to-fiber optical insertion loss of the modulator-to-detector link, P_I is the laser's CW optical output power, and r_d is the photodetector responsivity at DC. The terms ρ and ϕ express the amplitude ratio (between 0 and 1) and phase difference between the two balanced arms. For a perfect balance, $\rho = 1$ and $\phi = 0$, so that the total noise current spectral density of the detected *RIN* is zero. This suppression of the effect of the *RIN* is the primary advantage of the balanced link architecture.

In (1), the sum of the three noise current densities is divided by the link's intrinsic gain, g_i. Assuming R_{LOAD} is equal to the RF source impedance R_S, g_i for an external modulation link in which a quadrature-biased, balanced-output Mach-Zehnder modulator is optically connected to a balanced photodetector pair can be written as

$$g_i = \left[\frac{T_{FF}\,P_I\,\pi\,R_S}{4V_\pi(f)}\right]^2 \left(1+\rho^2+2\rho\cos\phi\right) r_d^2 \left|H_{D,dev}(f)\right|^2 \left|H_{D,pkg}(f)\right|^2, \quad (7)$$

in which $V_\pi(f)$ is the modulator's frequency-dependent switching voltage. For perfectly balanced modulator-to-detector paths, $1 + \rho^2 + 2\,\rho\cos\phi = 4$, and so

$$g_i = \left[\frac{T_{FF}\;P_I\;\pi\;R_S}{2\;V_\pi(f)}\right]^2 r_d^2\;\left|H_{D,dev}(f)\right|^2\;\left|H_{D,pkg}(f)\right|^2. \quad (8)$$

This potential boost in gain (by a factor of about 6 dB) is a secondary advantage of the balanced link architecture.

The frequency-dependent V_π of a modulator in which the velocity of a microwave signal along the traveling-wave electrodes matches that of the light in the waveguides has been derived previously [5]:

$$V_\pi(f) = V_\pi(DC)\,\frac{\alpha L}{1-e^{-\alpha L}}\;e^{\alpha_h L_h}, \quad (9)$$

where α_h and L_h are the attenuation coefficient and length, respectively, of any transmission line between the modulator input and the point at which the microwave and optical fields begin to interact, and where α and L apply over the region of microwave-optical interaction. It is important to note that a low $V_\pi(f)$—which is desirable, as shown in (8)—results from minimizing $\alpha(f)$, $\alpha_h(f)$, and L_h, but not from minimizing L, because $V_\pi(DC)$ is inversely proportional to this length.

From (1) – (9) it is clear that minimizing NF amounts to minimizing RIN, α, α_h, L_h, and ϕ, and to maximizing T_{FF}, P_I, r_d, $|H_D(f)|^2$, and ρ (to its maximum value of 1). The effect of L on NF is more complicated, as is discussed further (although only briefly) in Section III.B.

III. Link Component Selection

A. Laser

To achieve the desired power levels at λ = 1.55 μm, we considered only two optical sources: 1) a high-power distributed-feedback (DFB) diode laser, and 2) an Er-doped fiber laser oscillator followed by an Er-doped fiber amplifier. The CW 1.55 μm optical power that these lasers could deliver into their polarization-maintaining output fibers, P_I, was up to 250 mW for the DFB laser and up to 400 mW for the amplified doped-fiber laser. For the optical insertion loss (T_{FF}) and photodetector responsivity (r_d) that we expected for the link, only about 200 mW was necessary to achieve the desired amplitude of photocurrent in each detector.

Diode-pumped solid-state and doped-fiber lasers generally have lower *RIN* across microwave frequency bands than DFB and other diode lasers do. However the addition of an optical amplifier can worsen *RIN,* even when appropriate optical filters are used. We measured the *RIN* of the amplified doped-fiber laser and found it to vary between about −156 and −162 dB/Hz in the 1 – 10 GHz band. This was consistently higher than the *RIN* we measured for the high-power DFB diode laser, which was < −162 dB/Hz across this entire frequency band. We therefore decided to use the DFB as the laser in our link. It was our goal to use the noise cancellation feature of the balanced link architecture to suppress $\overline{i_{RIN}^2}$ to the extent that its effect on *NF* would be the same as if the laser *RIN* were < −180 dB/Hz—*i.e.*, a negligible effect.

B. Modulator

As shown in (8), the modulator parameters that affect g_i, and therefore *NF*, are its optical insertion loss—which usually dominates the total T_{FF} for an external modulation link—and its V_π. Whereas the modulator's insertion loss is simply inversely proportional to L, $V_\pi(f)$ is a more complicated function of L, decreasing with increasing L for small values of L, but asymptotically approaching a minimum value—determined by $\alpha(f)$ and $\alpha_h(f)\cdot L_h$—for large L. We used a modulator for which L was ~ 6.5 cm. This long microwave-optical interaction length, together with the dual-drive electrode configuration sketched in Fig. 2, enabled the modulator to exhibit a V_π of ~ 1.8 V at 6 GHz when measured from the input to the RF directional coupler using a two-tone IMD method [5]. The modulator's measured insertion loss was ~ 6 dB.

C. Photodetector

As established in Section II, a balanced photodetector is required for two reasons, the primary one being the reduction of the effect of *RIN* on the link *NF*, and the secondary one being the increase in g_i and consequently a further reduction in *NF*. From (8) it is also clear that we need the detector responsivity to be as high as possible and to degrade only negligibly over the desired bandwidth, because g_i is quadratically dependent on r_d, $H_{D,dev}(f)$, and $H_{D,pkg}(f)$. However, perhaps the single most important photodiode parameter in achieving a link with low noise figure is I_D, the average photocurrent. Three parameters contribute to the ability to have a large photocurrent: P_I, T_{FF} and r_d. Based on what we estimated we could obtain for these three parameters, and on the maximum photocurrents that we knew could be handled by broadband devices, we targeted a value of ~ 20 mA for I_D in this link design. When the laser, modulator, and balanced photodetector were optically connected, we measured I_D ~ 17 mA when the laser was biased for an output power of 187 mW. Increasing P_I to achieve larger I_D did not affect the measured link gain or noise figure.

IV. Results

For the link diagrammed in Fig. 2, Fig. 3 shows the measured and modeled intrinsic gain and noise figure vs. frequency. The modeled data were calculated using (1) – (8), assuming the device parameters listed below.

Laser: $P_I = 187$ mW
$RIN = -162$ dB/Hz (at worst, 1 – 10 GHz)

Modulator: $V_\pi(6\text{ GHz}) = 1.81$ V
$n = 2.14$

$$\alpha = \alpha_h = \alpha_0\sqrt{f} + \alpha_1 f$$

$$\alpha_0 = 0.019/\sqrt{\text{GHz}}\ \text{cm}$$

$$\alpha_1 = 0.0005/\text{GHz cm}$$

$L = 6.5$ cm
$L_h = 0.1$ cm

Detectors: $r_d = 0.81$ A/W
$|H_{D,dev}(f)|^2\ |H_{D,pkg}(f)|^2 = 0$ dB at DC
$= -0.1$ dB at 6 GHz
$= -3.5$ dB at 10 GHz

Optical link: $T_{FF} = -6.5$ dB
$\rho = -0.5$ dB
$\phi = 1°$ at 6 GHz

As can be seen from Fig. 3, there is only ~ 1 dB of disparity between the calculated and measured gains and noise figures at 1 GHz. An investigation into this discrepancy is under way; we suspect that we may not be accounting for all RF losses in the photodetector circuit. We also believe that the increase in the disparity between measured and modeled results at higher frequencies arises from a mismatch in the velocities of the optical and RF waves along the traveling-wave section of the modulator electrodes, and this is also being investigated with the help of a previously published model [5].

Acknowledgement

This material is based upon work supported by DARPA under SSC-San Diego Contract No. N66001-04-C-8045. Any opinions, findings and conclusions or recommendations expressed in this material are those of the authors and do not necessarily reflect the views of DARPA or SSC San Diego.

References

[1] C. Cox, *Analog Optical Links*, Cambridge University Press, 2005.

[2] E. Ackerman, C. Cox, G. Betts, H. Roussell, K. Ray, and F. O'Donnell, "Input impedance conditions for minimizing the noise figure of an analog optical link," *IEEE Trans. Microwave Theory Tech.,* vol. 46, pp. 2025-2031, December 1998.

[3] K. Williams, L. Nichols, and R. Esman, "Photodetector nonlinearity limitations on a high-dynamic range 3 GHz fiber optic link," *J. Lightwave Technol.*, vol. 16, pp. 192-199, February 1998.

[4] E. Ackerman and C. Cox, "The effect of a Mach-Zehnder modulator's traveling-wave electrode loss on a photonic link's noise figure," *Proc. IEEE International Topical Meeting on Microwave Photonics*, September 2003.

[5] G. Gopalakrishnan, W. Burns, R. McElhanon, C. Bulmer, and A. Greenblatt, "Performance and modeling of broadband $LiNbO_3$ traveling wave optical intensity modulators," *J. Lightwave Technol.*, vol. 12, pp. 1807-1819, October 1994.

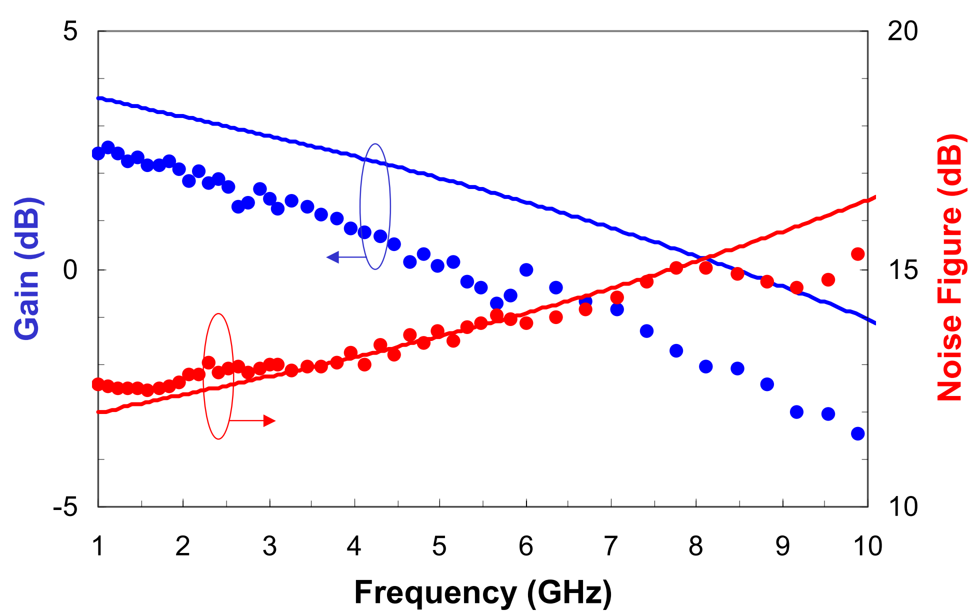

Fig. 3 Measured (points) and modeled (lines) link Gain and Noise Figure for the link diagrammed in Fig. 2. Parameters used in the model are listed in Section IV.